BUSING, W. R. & LEVY, H. A. (1964). *Acta Cryst.* **17**, 142–146.
FRITZ, I. J., GOTTLIEB, M., ISAACS, T. J. & MOROSIN, B. (1981). *J. Phys. Chem. Solids*, **42**, 269–273.
FRITZ, I. J., ISAACS, T. J., GOTTLIEB, M. & MOROSIN, B. (1978). *Solid State Commun.* **27**, 535–539.
GARBER, D. I. & KINSEY, R. R. (1976). *Neutron Cross Sections.* BNL 325, 3rd ed., Vol. III. Brookhaven National Laboratory, Upton, NY.
GOTTLIEB, M., ISAACS, T. J., FEICHTNER, J. D. & ROLAND, G. W. (1974). *J. Appl. Phys.* **45**, 5145–5151.
JOHNSON, C. K. (1976). *ORTEP*II. Report ORNL-5138. Oak Ridge National Laboratory, Tennessee.
KOESTER, L. & YELON, W. B. (1982). *Compilation of Low Energy Neutron Scattering Lengths and Cross Sections.* ECN, Netherlands Energy Research Foundation, Department of Physics.
LARSON, A. C. (1977). *Program and Abstracts.* American Crystallographic Association Summer Meeting, East Lansing, Michigan, paper H8, p. 67.
MUGHABGHAB, S. F. & GARBER, D. I. (1973). *Neutron Cross Sections.* BNL 325, 3rd ed., Vol. I. Brookhaven National Laboratory, Upton, NY.
SCHULTZ, A. J. (1984). Private communication.
VERGAMINI, P. J., LARSON, A. C. & ALKIRE, R. W. (1985). In preparation.

*Acta Cryst.* (1985). C**41**, 1714–1717

# Ammonium Trifluoroberyllate. High-Temperature Phases I and II

BY A. WAŚKOWSKA

*Institute of Low Temperature and Structure Research, Polish Academy of Sciences, 50–950 Wrocław, Pl. Katedralny 1, Poland*

(*Received* 15 *February* 1985; *accepted* 12 *August* 1985)

**Abstract.** $[NH_4][BeF_3]$, $M_r = 84{\cdot}05$; phase I: orthorhombic, *Pmnb*, $a = 5{\cdot}743\ (5)$, $b = 4{\cdot}643\ (5)$, $c = 12{\cdot}789\ (2)$ Å, $V = 341{\cdot}0\ (2)$ Å$^3$, $Z = 4$, $D_m = 1{\cdot}63\ (2)$, $D_x = 1{\cdot}637\ (3)$ Mg m$^{-3}$, $\lambda$(Mo $K\alpha$) $= 0{\cdot}7107$ Å, $\mu = 0{\cdot}94$ mm$^{-1}$, $F(000) = 168$, $T = 386$ K, final $R = 0{\cdot}057$ for 287 observed reflections; phase II: orthorhombic, $P2_12_12_1$, $a = 5{\cdot}661\ (4)$, $b = 4{\cdot}600\ (5)$, $c = 12{\cdot}990\ (3)$ Å, $V = 338{\cdot}3\ (4)$ Å$^3$, $Z = 4$, $D_x = 1{\cdot}650\ (3)$ Mg m$^{-3}$, $\lambda$(Cu $K\alpha$) $= 1{\cdot}5418$ Å, $\mu = 2{\cdot}04$ mm$^{-1}$, $T = 295$ K, final $R = 0{\cdot}051$ for 419 observed reflections. Phase II is metastable at room temperature which allowed data collection at room temperature. Both high-temperature phases are closely related to the ferroelastic phase III [Waśkowska (1983). *Acta Cryst.* C**39**, 1167–1169]. Rigid $BeF_4$ groups preserve nearly the same shape through the phase transition. Temperature-induced motion of the rigid molecular units leads to pronounced changes in conformation of the $(BeF_4)_n$ chains and through a system of hydrogen bonds of N—H···F type causes reorientation of $NH_4^+$ ions during phase transition.

**Introduction.** $NH_4BeF_3$ belongs to the family of ferroelastic hydrogen-bonded crystals and on heating undergoes phase transitions at $T_3 = 252{\cdot}2$, $T_2 = 334{\cdot}3$ and $T_1 = 347{\cdot}3$ K. At room temperature the crystal is ferroelastic (Makita & Suzuki, 1980; Czapla, Czupiński & Waśkowska, 1982). Thermogravimetric analysis, measurements of specific heat (DSC), X-ray studies of lattice parameters as a function of temperature, and Weissenberg photographs performed in temperature regions corresponding to particular phases led to the following phase diagram (Łukaszewicz, Waśkowska, Tomaszewski & Czapla, 1983):

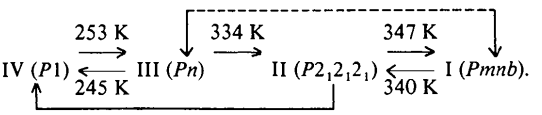


The crystals were grown from an aqueous solution of phase III. On heating, they transform at $T_2$ to the intermediate phase II. On cooling, the sequence of the phases is I → II → IV, *i.e.* phase II transforms directly to phase IV. Below room temperature both phases II and III transform at $T_3' = 245$ K to phase IV, which on heating returns to the room-temperature phase III. The X-ray crystal structure of the room-temperature phase was described by Waśkowska (1983). In the present paper the structures of the high-temperature phase I and of the intermediate phase II are determined and compared with the phase III in an attempt to find a molecular phase-transition mechanism in $NH_4BeF_3$.

**Experimental.** *Phase* I. Growth conditions described by Czapla *et al.* (1982). $D_m$ by flotation in dibromoethane/chloroform. Cylinder-shaped sample from the plate elongated in **b** ($r = 0{\cdot}15$, $l = 0{\cdot}37$ mm) heated to 358 (2) K. Lattice parameters from eight high-angle reflections in range $63{\cdot}3 \le \theta \le 82{\cdot}5°$ measured as function of temperature on a Bond diffractometer using Cu $K\alpha$ radiation (Łukaszewicz *et al.*, 1983). Stoe STADI-2 two-circle diffractometer (Mo $K\alpha$ radiation,

0108-2701/85/121714-04$01.50 

graphite monochromator). Data collection: $\omega$ scan, step-scan rate 0·01° s$^{-1}$, scan width 1·2°, background counts 20 s, $3° < \theta < 33°$. Two separate intensity sets: $A$ for $a$ rotation axis ($h$ 0 to 7, $k$ 0 to 6, $l$ −14 to 14) and $B$ for $b$ rotation axis ($h$ 0 to 7, $k$ 0 to 5, $l$ −14 to 14) gave a total of 1064 measured reflections. After averaging, 285 symmetry-independent reflections in $A$ and 249 in $B$ were corrected for Lp (absorption ignored) and brought to a common scale to produce a single set of 287 independent reflections ($R_{int} = 0·030$) with $|F| > \sigma(F_o)$. Standard reflections measured after every 20 reflections for each layer, variation ±4%. Space-group extinctions consistent with non-standard setting $Pmnb$ or $P2_1nb$ of space groups Nos. 62 or 33, which were chosen to correlate the high-temperature phase with the pseudo-orthorhombic room-temperature phase III. Structure solved on basis of atomic parameters of phase III. Full-matrix least-squares refinement (on $F$) in the space group $Pmnb$ led to $R = 0·057$; unit weights confirmed by analysis of variance of the mean $w\Delta^2$ with $F_o$; $S = 0·93$ for (27 +6 scales) variables. Max. and av. $\Delta/\sigma = 0·9$ and 0·03, respectively. N-bonded H atoms not located unequivocally and not included in calculations. Final difference Fourier map featureless, largest peaks 0·6 to 1·3 e Å$^{-3}$ around N. Extinction correction applied in the form: $F_c(1 + 2gF_c^2\Delta)^{-1/4}$, where $g$ converged to a value of $3·85 \times 10^{-3}$. Refinement in space group $P2_1nb$ stopped at $R = 0·24$ giving unsatisfactory model of $BeF_4$ tetrahedron, with large oscillating parameter shifts. Atomic scattering factors from Cromer & Mann (1968). Calculations with *XRAY*76 system (Stewart, Machin, Dickinson, Ammon, Heck & Flack, 1976).

*Phase* II. The particular effect of supercooling of phase II down to room temperature (Łukaszewicz *et al.*, 1983) made possible the data collection at room temperature. Plate elongated along **b**, ground to cylinder ($r = 0·16$, $l = 0·36$ mm), heated to 340 K on a Weissenberg camera equipped with a high-temperature furnace. Next cooled to room temperature and examined with respect to the space-group extinctions. Systematic absences consistent with $P2_12_12_1$. Philips PW 1100 diffractometer, monochromated Cu $K\alpha$, $\theta$–$2\theta$ scanning technique, scan range 1·2°, scan rate 0·04° s$^{-1}$. Lattice parameters from 18 reflections. 564 measured independent reflections ($h$ 0 to 7, $k$ 0 to 5, $l$ 0 to 16), $\sin\theta/\lambda_{max} = 0·62$ Å$^{-1}$. Lp correction applied, absorption ignored. 419 reflections with $|F| > \sigma(F_o)$ taken as observed. Three standard reflections, variation within 3%. Starting positional parameters taken from molecule (I) in phase III. H atoms located at the end of refinement from difference Fourier map and set at fixed positions with $U = 0·05$ Å$^2$. Full-matrix least-squares refinement on $|F|$ gave $R = 0·051$ and $wR = 0·055$, $w = 1/\sigma^2(F_o)$, $S = 0·56$ for 47 variables. Max. and av. $\Delta/\sigma$ ratios 0·1 and 0·02. Final residual map within 0·20 and 0·65 e Å$^{-3}$. Extinction correction $g = 4·25 \times 10^{-2}$. Atomic scattering factors for H atoms from Stewart, Davidson & Simpson (1965). Calculations performed using *XRAY*76 (Stewart *et al.*, 1976).

**Discussion.** The final atomic parameters for phases I and II are listed in Table 1.* Atomic arrangements of both phases are similar to that of the monoclinic phase (Waśkowska, 1983). The pattern of the structure consisting of long chains of $BeF_4$ tetrahedra parallel to the $b$ axis remains similar in all three phases (Fig. 1). Table 2 shows bond lengths and bond angles in the phases under investigation. Rigid tetrahedra preserve a type of deformation observed already in phase III with the same two Be—F distances elongated relative to the mean value of 1·526 (2) Å. Such a deformation implies the existence of stretching forces acting along the chain. The main difference between the structures involves temperature-induced conformational changes in $(BeF_4)_n$ chains which result from the different symmetries of particular phases (Fig. 1). The motion of $BeF_4$ tetrahedra influences, through a system of hydrogen bonds of N—H···F type, an environment of $NH_4^+$ ions, coordinated by eight F atoms, of which four are closer to the $NH_4^+$ ion than the others. N—F distances vary as shown in Table 3, where the shortest and the longest distances are compared for subsequent phases. The discrepancy $\Delta$ between the longest and the shortest N—F contacts is smaller in phase I, and increases with decreasing symmetry in phases II and III.

It is possible to discuss the molecular transition model in terms of deformation of prototype (aristotype) phase I. The transition to the low-temperature phase is connected with deviations of structural elements from the high-symmetry positions.

Conformational differences along the $(BeF_4)_n$ chain are shown in Fig. 1. Heavy lines denote positions of tetrahedra in phase I. The space-group symmetry requires the $BeF_4^-$ and $NH_4^+$ tetrahedra to lie on the mirror planes at $y = \frac{1}{4}$ and $\frac{3}{4}$. Comparison of $U_{ij}$ values for F(11) and F(12) suggests that r.m.s. displacements of the vertex at F(12) are about three times larger than those of F(11), which means that translational motion of tetrahedra along the chain is much less pronounced than rotational motion or rotational disorder around the axis running through the F(11)—F(11′) *etc.* vertices. In phase II (dashed lines) edges sharing common corners are no longer in line with the chain axis. The angle between the two edges is 165°. Highly anisotropic values of the thermal parameters of all the F atoms, in comparison to those of the Be atom, mean that besides rotational motion, tilting of the tetrahedra relative to

* Lists of structure factors, anisotropic thermal parameters, N—F distances and details of hydrogen bonds have been deposited with the British Library Lending Division as Supplementary Publication No. SUP 42447 (9 pp.). Copies may be obtained through The Executive Secretary, International Union of Crystallography, 5 Abbey Square, Chester CH1 2HU, England.

each other along the chain also occurs. The behaviour of these rigid groups is similar in phase III (dotted lines), with the difference that the angle between the edges connecting the vertices at the F(11) atoms is 174°.

In Fig. 2 are shown the changes in the arrangement of the chains in the unit cell for subsequent phases. In the transition at $T_1$ each of the two chains of tetrahedra rotates around **b** in opposite directions relative to the symmetry-constrained positions in phase I by about 9° (Fig. 2). In phase III a reorientation of the chains takes place, both chains being rotated in the same direction by about 9° relative to phase I.

Table 1. *Positional and thermal parameters with e.s.d.'s in parentheses*

$U_{eq} = (U_{11} + U_{22} + U_{33})/3$. For H atoms $U_{iso}$ is given. The atom numbering is the same as that used for the room-temperature phase.

| | $x$ | $y$ | $z$ | $U_{eq}$(Å$^2$ × 10$^2$) |
|---|---|---|---|---|
| Phase I | | | | |
| N | 0·7500 | 0·7287 (1) | 0·09608 (5) | 1·84 (4) |
| Be | 0·2500 | 0·1773 (2) | 0·18153 (8) | 1·61 (6) |
| F(11) | 0·2500 | −0·13887 (9) | 0·21579 (3) | 2·50 (3) |
| F(12) | 0·4540 (1) | 0·2368 (1) | 0·11843 (4) | 7·19 (4) |
| Phase II | | | | |
| N | 0·7041 (7) | 0·7252 (9) | 0·1001 (3) | 3·3 (2) |
| Be | 0·2015 (9) | 0·1775 (9) | 0·1858 (4) | 2·4 (3) |
| F(11) | 0·2277 (6) | −0·1561 (5) | 0·2141 (2) | 3·3 (1) |
| F(12) | 0·3667 (5) | 0·2474 (7) | 0·0986 (2) | 4·3 (2) |
| F(13) | −0·0554 (4) | 0·2333 (7) | 0·1622 (3) | 5·4 (1) |
| H(1) | 0·739 | 0·730 | 0·026 | 4·93 |
| H(2) | 0·779 | 0·562 | 0·131 | 5·06 |
| H(3) | 0·782 | 0·904 | 0·127 | 6·31 |
| H(4) | 0·536 | 0·746 | 0·117 | 6·34 |

Table 2. *Bond lengths* (Å) *and bond angles* (°) *in* $BeF_4$ *tetrahedra*

In phase I the e.s.d.'s are in parentheses; in phase II the e.s.d.'s are 0·006 Å for distances and 0·04° for angles.

| Phase I | | Phase II | |
|---|---|---|---|
| Be–F(11) | 1·532 (2) | Be–F(11) | 1·585 |
| Be–F(12) | 1·449 (1) | Be–F(12) | 1·503 |
| Be–F(12$^{i}$) | 1·449 (1) | Be–F(13) | 1·508 |
| Be–F(11$^{ii}$) | 1·566 (1) | Be–F(11$^{iii}$) | 1·561 |
| F(11)–Be–F(12) | 110·00 (5) | F(11)–Be–F(12) | 108·9 |
| F(11)–Be–F(12$^{i}$) | 110·00 (5) | F(11)–Be–F(13) | 107·6 |
| F(11)–Be–F(11$^{ii}$) | 106·41 (8) | F(11$^{iii}$)–Be–F(11) | 104·9 |
| F(12)–Be–F(12$^{i}$) | 107·89 (9) | F(12)–Be–F(13) | 114·2 |
| F(12)–Be–F(11$^{i}$) | 111·27 (5) | F(12)–Be–F(11$^{iii}$) | 111·3 |
| F(12)–Be–F(11$^{i}$) | 111·27 (6) | F(13)–Be–F(11$^{iii}$) | 109·5 |

Symmetry code: (i) $\frac{1}{2}-x, y, z$; (ii) $x, \frac{1}{2}+y, \frac{1}{2}-z$; (iii) $\frac{1}{2}-x, \frac{1}{2}+y, \frac{1}{2}-z$.

Table 3. *The shortest and the longest* N–F *distances in particular phases.*

| Phase | N–F distances (Å) Shortest | Longest | $\Delta$ (Å) |
|---|---|---|---|
| I | 2·861 (3) | 3·312 (2) | 0·451 |
| II | 2·743 (5) | 3·359 (2) | 0·616 |
| III | 2·755 (1) | 3·435 (1) | 0·680 |

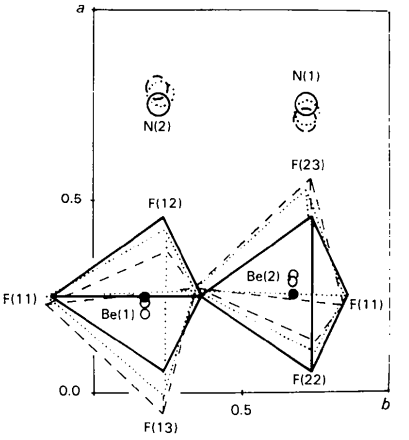


Fig. 1. Temperature-induced changes of $(BeF_4)_n$ chains resulting from different symmetry in subsequent phases. (Phase I heavy lines, II dashed lines, III dotted lines.)

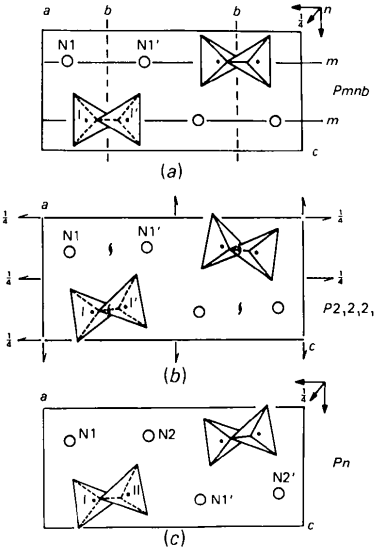


Fig. 2. Tilting of structural elements from positions of phase I during phase transitions: (*a*) prototype high-symmetry phase (*Pmnb*); (*b*) intermediate phase I ($P2_12_12_1$); (*c*) ferroelastic phase III (*Pn*).

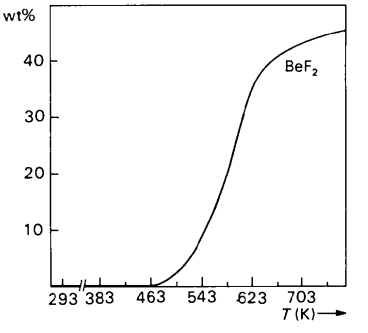


Fig. 3. Thermogravimetric analysis of $NH_4BeF_3$ crystals (sample weight 35 mg).

In our earlier paper (Łukaszewicz *et al.*, 1983) we reported that in some crystals of $NH_4BeF_3$ grown from the same mother solution phase II was missing, which we attributed to differences in crystal perfection and the distribution of defects. The intermediate phase II was also not found by Makita & Suzuki (1980), Yoshida, Tsukamoto, Futama & Makita (1984) or Yoshida, Takemasa, Oshino & Makita (1984). It should be added that the transition at 526 K reported by Yoshida, Tsukamoto *et al.* (1984) and Yoshida, Takemasa *et al.* (1984) is not connected with an additional phase transition but corresponds to decomposition of the compound. Thermogravimetric analysis (Fig. 3) performed on an Elmer–Perkin gravimeter shows that at 471 K a loss of weight of sample starts according to the scheme: $NH_4BeF_3 \rightarrow NH_4F + BeF_2$. This effect was also observed on the DSC curve where a broad and irregular peak, typical for decomposition of the substance, was recorded at the same temperature.

The author thanks Professor K. Łukaszewicz for his constant interest and for critically reading the manuscript, Dr Z. Czapla, University of Wrocław, for supplying crystals, Professor L. Kihlborg, Arrhenius Laboratory, Stockholm, for providing facilities for the use of the PW 1100 diffractometer, Dr T. Niklewski, also from Arrhenius Laboratory, for gravimetric analysis, and Dr M. Wołcyrz and W. Paciorek from our institute for valuable discussions.

### References

CROMER, D. T. & MANN, J. B. (1968). *Acta Cryst.* A**24**, 321–324.
CZAPLA, Z., CZUPIŃSKI, O. & WAŚKOWSKA, A. (1982). *J. Phys. Soc. Jpn*, **51**, 2693–2694.
ŁUKASZEWICZ, K., WAŚKOWSKA, A., TOMASZEWSKI, P. E. & CZAPLA, Z. (1983). *Phase Transitions*, **4**, 47–54.
MAKITA, Y. & SUZUKI, S. (1980). *J. Phys. Soc. Jpn*, **48**, 693–694.
STEWART, J. M., MACHIN, P. A., DICKINSON, C. W., AMMON, H. L., HECK, H. & FLACK, H. (1976). The *XRAY*76 system. Tech. Rep. TR-446. Computer Science Center, Univ. of Maryland, College Park, Maryland.
STEWART, R. F., DAVIDSON, E. R. & SIMPSON, W. T. (1965). *J. Chem. Phys.* **42**, 3175–3187.
WAŚKOWSKA, A. (1983). *Acta Cryst.* C**39**, 1167–1169.
YOSHIDA, H., TAKEMASA, H., OSHINO, Y. & MAKITA, Y. (1984). *J. Phys. Soc. Jpn*, **53**, 2600–2605.
YOSHIDA, H., TSUKAMOTO, T., FUTAMA, H. & MAKITA, Y. (1984). *J. Phys. Soc. Jpn*, **53**, 2606–2612.

*Acta Cryst.* (1985). C**41**, 1717–1718

# Structure of Tribarium Dibismuth Tetrakis(phosphate)

BY R. MASSE AND A. DURIF

*Laboratoire de Cristallographie, Centre National de la Recherche Scientifique, Laboratoire associé à l'USMG, 166 X, 38042 Grenoble CEDEX, France*

(*Received* 12 *June* 1985; *accepted* 29 *August* 1985)

**Abstract.** $Ba_3Bi_2(PO_4)_4$, $M_r = 1209{\cdot}87$, monoclinic, $C2/c$, $a = 20{\cdot}298$ (20), $b = 8{\cdot}730$ (3), $c = 8{\cdot}766$ (3) Å, $\beta = 109{\cdot}98$ (6)°, $V = 1460{\cdot}0$ (7) Å$^3$, $Z = 4$, $D_x = 5{\cdot}504$ Mg m$^{-3}$, Ag $K\alpha_1$, $\lambda = 0{\cdot}56083$ Å, $\mu = 176{\cdot}7$ cm$^{-1}$, $F(000) = 2088$, $T = 293$ K, $R = 0{\cdot}038$, 3036 unique reflections. Isolated $PO_4$ tetrahedra determine irregular coordinations around Ba and Bi atoms. The sites of Ba(1) and Ba(2) have eightfold coordination with a more regular arrangement around Ba(2), which is in a special position. The Bi atom has seven oxygen neighbours in a distorted arrangement.

**Introduction.** The monophosphate $Ba_3Bi_2(PO_4)_4$ was prepared starting from a $Ba(PO_3)_2$,$2Bi_2O_3$ mixture, melted at 1373 K and cooled slowly to 1173 K and then rapidly to room temperature. The initial aim was to obtain a chemical compound with the $BiO_5$ pyramidal arrangement.

**Experimental.** Thick platelet: 0·16 × 0·24 × 0·24 mm. Weissenberg photographs and data collection indicate monoclinic symmetry ($hkl$, $h+k = 2n$ and $h0l$, $l = 2n$) compatible with space groups $Cc$ and $C2/c$; cell constants from 20 reflections ($10 < \theta_r < 13°$) using a four-circle Philips PW 1100 diffractometer. Graphite-monochromated Ag $K\alpha$, $\omega/2\theta$ scan, scan width 1·2°, scan speed 0·02° s$^{-1}$. $\theta$ range 3 to 35°. $\pm h,k,l$, $h_{max} = 45$, $k_{max} = 30$, $l_{max} = 30$. Intensity reference reflections 060 and 462. 4985 independent reflections collected. 3036 ($F_o > 2\sigma_F$) used to refine structure until $R = 0{\cdot}038$, $wR = 0{\cdot}048$; unit weights; full-matrix refinement on $F$; no absorption correction; structure solved using three-dimensional Patterson function, followed by successive Fourier syntheses. $S = 4{\cdot}84$. Max. $\Delta/\sigma = 0{\cdot}02$ (scale factor). Residual electron density peaks $< 3{\cdot}1$ e Å$^{-3}$. Atomic scattering factors and $f'$ and $f''$ values from *International Tables for*

0108-2701/85/121717-02$01.50